Catalysis Letters 15 (1992) 189–197

Platinum sintering inhibition by yttrium oxide

Bob R. Powell

Metallurgy Department, General Motors Research Laboratories, Warren, MI 48090-9055, USA

Mixtures of yttrium oxide and platinum powders undergo a chemical interaction that inhibits the sintering of the mixture, thereby stabilizing its open pore network at temperatures up to 1500°C. A mechanism for this phenomenon has been proposed, based on the results of SEM, EPMA, and AES analysis. Sintering of the platinum particles beyond the intermediate stage (continuous pore channel) is inhibited by the formation of an yttrium-rich phase on the surface of the particles. The formation of this phase involves the wetting and spreading of yttrium oxide, initially present as 0.4 μm particles in the platinum. Spreading of yttrium oxide over the platinum inhibits sintering by lowering the surface energy of the platinum.

Keywords: Sintering; sensors; platinum; yttrium oxide; SMSI; surface interaction

1. Introduction

Platinum electrodes in gas sensors require a continuous, open pore network for high sensitivity and response. Unfortunately, the openness of the pore network can be destroyed if Pt particle sintering is too extensive. This can happen if the sensor is fabricated by co-firing; i.e., the platinum ink and zirconium dioxide (ZrO_2) substrate are fired at the same time. The co-fire temperature for Pt/ZrO_2 is approximately 1500°C.

Yttrium oxide (Y_2O_3) powder additions to the Pt have been shown to increase the stability of the Pt pore network, i.e., inhibit its sintering. The continuous pore network was retained even after sintering at 1510°C. The present study was undertaken to determine the nature of this beneficial Pt/Y_2O_3 interaction.

2. Experimental

Two sensor specimens with Pt electrodes containing Y_2O_3 additions were analyzed. The components of the sensor electrodes are described in table 1. Both sets of electrodes were prepared from inks containing Pt powder and 12.5 wt% Y_2O_3 powder. The main difference between the inks was the Pt powder

Table 1
Ink compositions and particle sizes used to prepare the samples

Ink component	Sample 1	Sample 2
Pt (particle diameter) (87.5 w/o)	75% (0.5–1.2 μm) 25% (0.1–0.4 μm)	100% (0.5–1.2 μm)
Y_2O_3 (particle diameter) (12.5 w/o)	(0.4 μm)	(0.4 μm)

used to prepare them. The Pt powder used in sensor 1 had a bimodal particle size distribution. The Pt used in sensor 2 was unimodally size distributed. After depositing the electrodes, the assembled sensors were sintered (co-fired) in air for 1 h at 1510°C.

The specimens were analyzed by scanning electron microscopy (SEM) with energy dispersive (EDS) and wavelength dispersive spectroscopies, by electron probe microanalysis (EPMA) and by Auger electron spectroscopy (AES). Both fracture cross-sections and polished cross-sections were inspected. The specimen for AES was oxidized at 780°C to remove carbon contamination. Fracture of this specimen was done in situ to prevent additional contamination.

3. Results

3.1. SCANNING ELECTRON MICROSCOPE ANALYSIS OF THE EXTERNAL SURFACE

The microstructure of the Pt electrode of sensor 1 is shown in fig. 1. Its open porosity Pt is evident. Platinum sintering has terminated after the initial stage; neck growth. All EDS spectra contained Pt as the major species with trace amounts of Y. Discrete particles of Y_2O_3 are absent. The particles of Y_2O_3 were originally 0.4 μm in diameter and, if present, should have been distinguishable in fig. 1, particularly since they would have occupied 35% of the material volume.

The surface of the platinum particles appears to be textured, fig. 1A, with regions of high (bright) and low (dark) contrast, fig. 1B. The bright regions are composed of higher atomic number elements than the dark regions, suggesting that they are Pt-rich and Y-rich, respectively. The same observations were made for sensor 2.

3.2. ELECTRON PROBE MICROANALYSIS OF POLISHED CROSS-SECTIONS

To acquire a better understanding of chemistry in the pore network, polished cross-sections of the samples were analyzed by EPMA. This technique was used

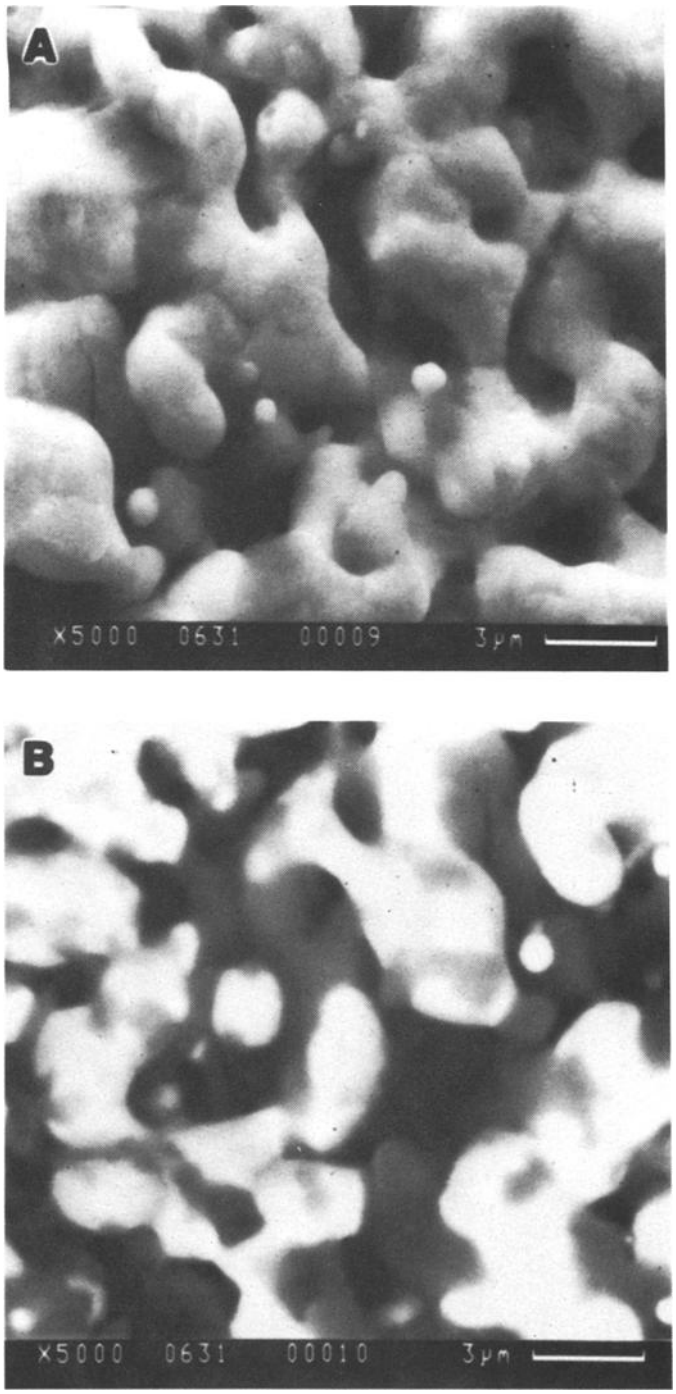

Fig. 1. Scanning electron micrographs (5000×) of the Pt electrode. Note the surface texture in (A). The backscattered image (B) reveals the differences in composition; bright areas corresponding to the higher atomic number element (Pt).

because of its ability to provide information about the elemental distributions that was not obtainable by SEM/EDS. A cross-section of the electrode in sensor 2 is shown in fig. 2. A portion of the ZrO_2 substrate is indicated. As before, the sample contains bright areas and dark areas. However, in this specimen, polishing marks are found to cross the bright areas, but not the dark areas. This suggests that bright areas in the sample are actually cross-sections of Pt network, while the dark areas, which are Y-rich, are the walls of the pore network. This interpretation was supported by stereo-pairs which show the bright areas to be flat and at the surface of the cross-section, whereas the dark areas are cavernous and recessed into the sample.

EPMA provides further evidence that the pore walls are Y-rich. Fig. 3A is a backscattered electron image of a polished cross-section. The Y elemental map of the cross-section is shown in fig. 3B. The particle in fig. 3A is Pt and the Y map shows that pore network walls around it contain Y. However, when compositions were determined, it was not possible to show that the Y concentration in the pore walls was different from that in the Pt particle cross-sections. This result suggested that the pore walls might be surface-rich in Y.

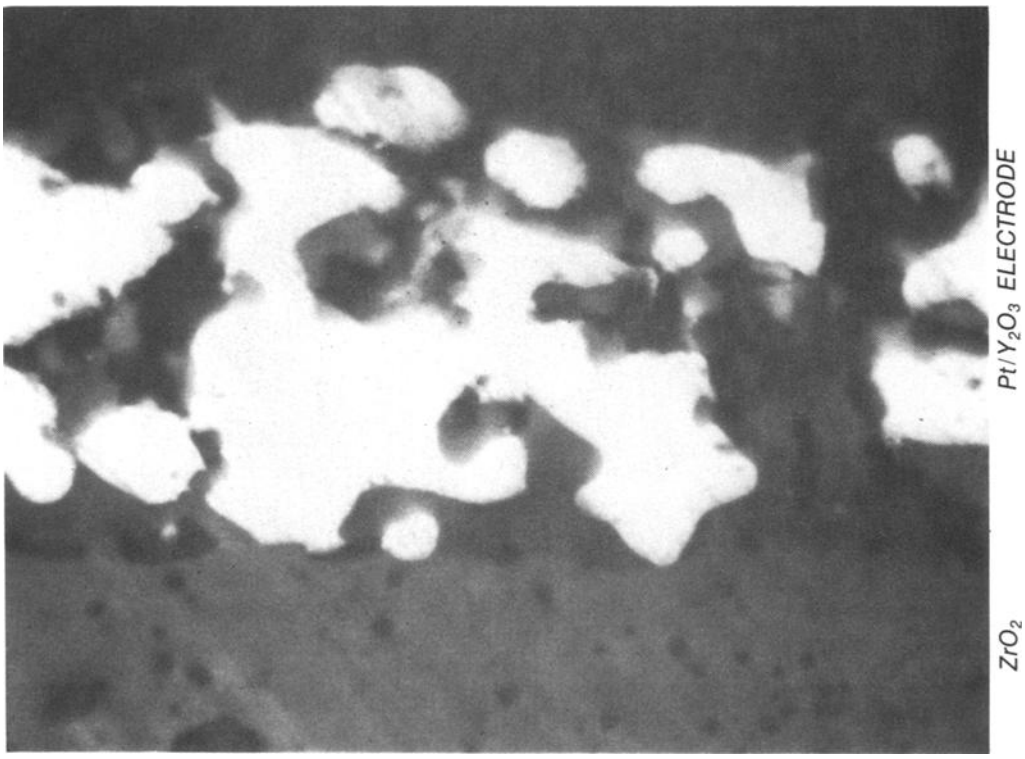

Fig. 2. Backscattered electron image (5000×) of a polished cross-section of the Pt electrode of sensor 2. The zirconium dioxide substrate is indicated in the figure.

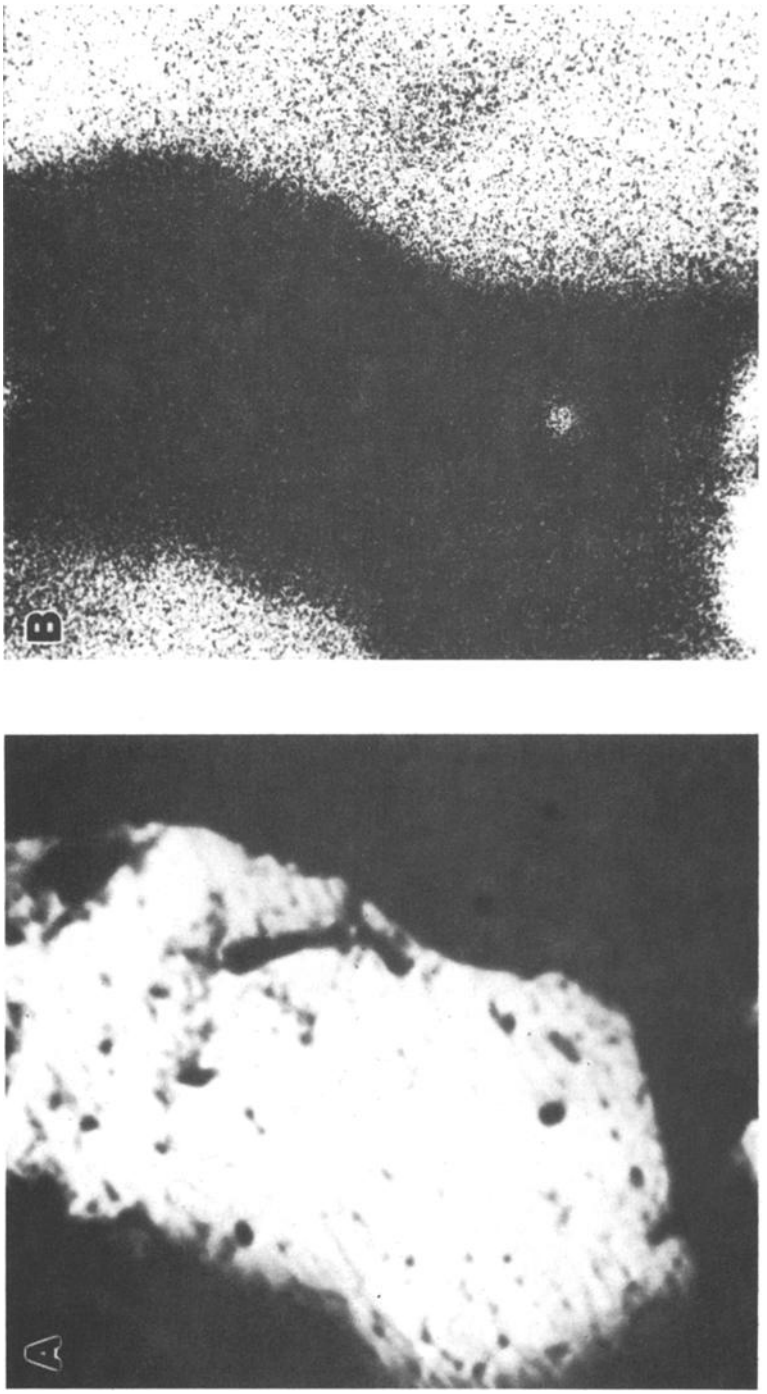

Fig. 3. Backscattered electron micrograph (BEI) and yttrium elemental map of a polished section of the Pt electrode of sensor 2. Magnifications are 8000×.

3.3. AUGER ELECTRON SPECTROSCOPY OF SPECIMENS FRACTURED IN SITU

AES is a surface sensitive chemical probe. Using this technique one can determine the chemical composition of a sample within 5 nm of its surface. AES was used to analyze a fracture surface of sensor 2. The fracture process was performed in situ. AES was performed on the as-fractured surface and again after ion sputter etching.

The approximate surface compositions, in at%, for selected regions of the specimen are given in table 2. These compositions are approximate because of uncertainties in the sensitivity factors for Pt, Y, and O, which were used in the calculations. Carbon content is low, indicating that the specimen treatment procedure was successful. The indium signal is due to an indium foil which was placed in the fracture stage to provide electrical contact between the sample strip and the spectrometer. Ion sputtering caused the indium to coat the specimen. The atomic compositions shown in table 2 were adjusted by treating carbon and indium as surface films. The new compositions, after eliminating these contaminants are shown in table 3.

The AES image of the as-fractured surface contains light and dark areas. These correspond to the Pt particle cross-sections and the pore network walls, respectively. Table 3 shows that the cross-sections are Pt-rich, although some Y was detected. The atomic composition in these areas is similar to what would be predicted for the overall composition of the sample, see footnote in table 3. Platinum was not detected in the pore network walls. Instead, the walls are probably Y_2O_3. EDS analysis detected Pt and Y, but then, the EDS probe penetrates deeper into the sample than does the AES probe, thus detecting sub-surface Pt that was not detected by the AES probe.

Table 2
Sample 2 composition based on Auger electron spectroscopy

Region	Thickness removed by etching (nm)	Composition (at%)			
		Pt	Y	O	other
cross-section	0	52	15	14	C-20
cross-section	0	41	27	31	
pore wall	0	–	47	51	In?-2
pore wall	0	–	34	66	
cross-section	5	14	21	61	In-3
cross-section	5	47	10	42	
pore wall	5	25	21	51	Ca?-3
pore wall	5	11	24	58	In-7
cross-section	55	26	18	38	In-18
pore wall	55	9	14	45	In-31

Table 3
Sample compositions based on Auger electron spectroscopy [a]

Cross-section			Network wall		
Pt	Y	O	Pt	Y	O
as fractured					
65	18	17	–	48	52
41	27	31	–	34	66
5 nm removed by sputter etching					
16	22	62	26	22	52
48	10	42	12	26	62
55 nm removed by sputter etching					
32	22	46	14	20	66
predicted a/o in starting material			Pt-60, Y-16, O-24		
predicted a/o in $Y_2Pt_2O_7$			Pt-18, Y-18, O-64		

[a] Composition reported as a/o after adjusting for carbon and indium contamination.

The Y_2O_3 on the pore network walls is a surface phase, because it is removed by ion sputter etching. Once approximately 5 nm of the surface has been removed, the concentration is actually close to that of $Y_2Pt_2O_7$, the pyrochlore-type oxide [1]. Removal of an additional 55 nm from the network wall does not alter its composition.

Sputter etching does not affect the measured composition of the Pt particle cross-sections. This suggests that its composition is more representative of the bulk of the sample. However, except for the as-fractured cross-section, the composition rarely approaches the known initial composition of the sample. The apparent deficiency of Pt is not due to volatility, the vapor pressure Pt being about 10^{-6} Torr at the sintering temperature. Nor was there evidence that Pt diffused into the zirconia electrolyte.

Despite some differences in conclusions from the different analytical tools, it is apparent that there are two phases present in the sample. One is Pt-rich and one is Y-rich (possibly pure Y or Y_2O_3). The fact that the Y-rich phase is observed only in the unetched sample, suggests that it is a surface phase.

4. Discussion

Based on these analyses, it is concluded that Y_2O_3 stabilizes the pore network of the sample by forming an Y-rich surface phase. The Y_2O_3 particles wet and spread over the Pt surfaces at the same time that the Pt is undergoing the initial stage of sintering, neck growth. Wetting and spreading apparently lower the surface free energy of the Pt, thereby reducing the driving force for continuation of the sintering process.

There is an analogue between the behavior of the Pt/Y_2O_3 system, that was observed in this work, and a phenomenon described in the catalysis literature: strong metal–support interactions (SMSI). The most well-understood example of SMSI is the observed migration of reduced titania (TiO_{2-x}) onto the surface of catalytic metals such as Ni [2], Rh [3], and Pt [4]. The resulting "surface oxide" alters the chemisorptive capacity of the catalytic metal, as well as its catalytic activity and selectivity. The reduction in chemisorptive capacity was the first observation that led to the recognition of the SMSI effect.

In the case of titania, it is believed that reduction of the oxide is necessary for the formation of the oxide film over the metal. This is consistent with the early experience with the SMSI effect in that the effect was limited to "easily reducible oxides" such as TiO_2, Ta_2O_5, and V_2O_5, but not present in more stable oxides such as Al_2O_3, SiO_2, ZrO_2, Sc_2O_3, MgO, and HfO_2 [5,6]. Y_2O_3 is one of the most stable oxides with respect to reduction, so it is surprising that this oxide should display the SMSI effect, especially when the SMSI effect was not observed when it was sought for in the early studies [6]. However, in this early work [5,6], the criterion of SMSI was reduced chemisorptive capacity. Surface oxide formation may still occur in these materials, but probably not without affecting chemisorptive capacity. Moreover, reduction of another very stable oxide, La_2O_3, has recently been observed in the presence of Pd [7,8]. Thus the results of the present work suggest that Y_2O_3 may yet be a member of the SMSI class of materials, at least with respect to the formation of a surface oxide. Considering its stabilizing effect on the Pt pore network, it may be revealing to evaluate other oxides, especially the SMSI oxides, for their possible roles in inhibition of Pt particle sintering. Also, the stabilizing effect of Y_2O_3 in the Pt system may be beneficial from a pore network perspective, but its effect on certain aspects of catalysis remains unknown.

5. Conclusions

Microscopic and spectroscopic analyses have led to an understanding of important microstructural changes in the Pt/Y_2O_3 samples:

(1) Y_2O_3, initially present as 0.4 μm particles in the Pt, forms an yttrium-rich surface phase within the Pt-pore network.

(2) The formation of this surface phase must therefore lower the overall surface energy of the sample system, thereby reducing the driving force for sintering of the porous Pt network.

(3) The advantage of this interaction is that, by hindering the sintering process, the openness of the pore network is stabilized during thermal processing steps that are necessary for fabrication of the sensor. This is important because an open pore network is essential for effective sensor operation.

(4) There is a phenomenological similarity of the Pt/Y_2O_3 interaction to aspects of the SMSI effect reported in the catalysis literature. A possible ramification of this is that while the Pt pore network is stabilized by the Y_2O_3, an influence of the Y_2O_3 on the catalytic properties of the Pt may also occur.

Acknowledgement

The author gratefully acknowledges discussions with Dr. Frederick Kennard (AC Rochester Division of General Motors) and Richard H. Hammar and Ken M. Rahmoeller (GM Research Laboratories). AC Rochester also provided the sensor specimens for this work. The author appreciates experimental contributions from James B. Walker and Curtis A. Wong for the scanning electron microscopy, Richard A. Waldo for the electron probe microanalysis, Steven J. Simko for performing the Auger electron spectroscopy experiments, and Raymond L. Bloink for sample preparation.

References

[1] H.R. Hoekstra and F. Gallagher, Inorg. Chem. 7 (1968) 2553.
[2] A.J. Simoens, R.T.K. Baker, D.J. Dwyer, C.R.F. Lund and R.J. Madon, J. Catal. 86 (1984) 359.
[3] D.N. Belton, Y.-M. Sun and J.M. White, J. Am. Chem. Soc. 106 (1984) 3059.
[4] D.J. Dwyer, J.L. Robbins, S.D. Cameron, N. Dudash and J. Hardenbergh, in: *Strong Metal–Support Interactions*, eds. R.T.K. Baker, S.J. Tauster and J.A. Dumesic (Am. Chem. Soc., Washington, 1986) pp. 21–33.
[5] S.J. Tauster and S.C. Fung, J. Catal. 55 (1978) 29.
[6] S.J. Tauster, S.C. Fung, R.T.K. Baker and J.A. Horsley, Science 211 (1981) 1121.
[7] T.H. Fleisch, R.F. Hicks and A.T. Bell, J. Catal. 87 (1984) 398.
[8] R.F. Hicks, Q.-J. Yen and A.T. Bell, J. Catal. 89 (1984) 498.